

Solvent content of protein crystals from diffraction intensities by Independent Component Analysis

Massimo Ladisa^a

*Istituto di Cristallografia-CNR, c/o Dipartimento Geomineralogico,
Università degli Studi di Bari, via E. Orabona 4, I-70125 Bari, Italy*

Antonio Lamura

Istituto Applicazioni Calcolo-CNR, sezione di Bari, via G. Amendola 122/D, I-70126 Bari, Italy

Giovanni Nico

*Istituto di Radioastronomia-CNR, sezione di Matera,
c/o Centro di Geodesia Spaziale-ASI, I-75100 Matera, Italy*

Dritan Siliqi

*Faculty of Natural Sciences, Department of Inorganic Chemistry,
Laboratory of X-ray Diffraction, Tirana 5, Albania*

(Dated: October 30, 2018)

An analysis of the protein content of several crystal forms of proteins has been performed. We apply a new numerical technique, the Independent Component Analysis (ICA), to determine the volume fraction of the asymmetric unit occupied by the protein. This technique requires only the crystallographic data of structure factors as input.

^a Corresponding author, E-mail: massimo.ladisa@ic.cnr.it, Phone: +39 0805442419, Fax: +39 0805442591

SHORT TITLE: ICA in protein crystallography

KEYWORDS: Matthews coefficient, protein crystallography, structure factors, solvent fraction, ICA algorithm

INTRODUCTION

Protein crystals contain between around 30% and 70% of solvent [1], most of which is disordered in the solvent channels among the protein molecules of the crystal lattice. Thus the electron densities of the protein molecules, with typical values of $0.43 \text{ e}/\text{\AA}^3$, are surrounded by a continuous disordered solvent electron density ranging between $0.33 \text{ e}/\text{\AA}^3$ for pure water and $0.41 \text{ e}/\text{\AA}^3$ for 4M ammonium sulphate [2].

If we do not account for any model for this continuous disordered solvent electron density, atomic protein models are thought as if it were placed in vacuum. The electron density itself is overestimated, the calculated structure factor amplitudes are systematically much larger than the observed ones [3], and it is commonly believed that the latter condition especially occurs at low resolution.

The higher is the discrepancy among the calculated structure factors and the observed ones, the more difficult is the data scaling, the least-square refinement and the electron density map rendering. Cutting low resolution data has been a widely adopted method to step over the problem, although it was rough and, somehow, intrinsically wrong: Indeed, it introduced distortions of the local electron density (an optical example is discussed in [4]).

A great effort has been recently devoted to devise a reliable method accounting for the disordered solvent effects in the protein region [5, 6]. Two of them deserve a brief description.

I. The exponential scaling model [7].

This model is obtained by the direct application of Babinet's principle to the calculated structure factors. The solvent structure factors moduli are assumed to be proportional to the protein ones, whereas the phases are opposite. The lower is the resolution the more satisfactory is the agreement between the observed structure factor and the calculated one [8]. Due to its simplicity, this model has been implemented in most of the crystallographic refinement programs [9]. The weakness of this model is strictly related to the resolution at which it is expected to work properly. Indeed the approximation embodied in this method is true at resolutions below $\approx 15\text{\AA}$ although it can be stretched up to $\approx 5\text{\AA}$ by downscaling the structure factors.

II. The mask model [10].

This model is an improvement of the previous one, since it aims to sum up the protein structure factor and the solvent one vectorially, *i.e.* by accounting for both the modulus and the phase of the two structure factors. In

the mask model the protein molecules are placed on a grid in the unit cell whereas the grid points outside the protein region are filled with the disordered solvent electron density. The protein boundary is mainly determined by the Van-der-Waals radii. The disordered solvent electron density is "stretched" to fill in the empty space and the calculation of the solvent structure factor is straightforward. Although the mask model works rather well, there are three major drawbacks of it: Too many parameters have to be fitted and the relatively large *parameters/observables* ratio weakens the model at high resolution (overfitting); finally, the disordered solvent electron density is unrealistically assumed to be step shaped and flat. Some strategies have been already devised to improve the latter ones [10].

The aim of this paper is to focus on a recently developed statistical method and its application to disentangle the protein and the solvent contributions out of crystallographic data; we show its major advantages and drawbacks. Up to our knowledge this method has never been applied to this field. A comparison of the protein fraction in the unit cell, calculated by this method, with the same quantity computed by the most popular method used nowadays [1] is satisfactory.

The plan of the paper is as follows: The *theory* section provides the reader with the basic concepts of the independent component analysis; the *results and discussion* section applies the theory to the specific case of a 2-dimensional problem (*i.e.* solvent/protein system) we are interested in; it concludes with the calculation of the protein fraction for several protein structures and with a comparison of this quantity with the analogous one calculated by the Matthews' model accounting for the protein content only. *Conclusions* section summarizes the paper's content and suggests further investigations.

THEORY

Several techniques have been devised so far to deal with protein crystallography. Among them we quote the isomorphous derivative (SIR, MIR) and the anomalous dispersion (SAD, MAD) ones (we address the reader to a number of review papers for details on these techniques; see, for instance, [11] and references therein).

The theory described hereafter can be applied to protein crystallography regardless of the specific technique we are using and without any substantial modification; therefore, for the sake of simplicity, we shall focus on the isomorphous derivative one. Anyway the method will be finally applied to several proteins: Among them some are anomalous dispersion structures and some others refer to the isomorphous derivative technique.

A protein and its isomorphous derivatives crystallize in a solvent. Imagine that you are measuring the diffraction intensities out of a crystallized protein sample and one of its isomorphous derivatives. Each of these recorded signals is a weighted sum of the signals emitted by the two main sources (*i.e.* protein/derivative and solvent), which we denote by $\mathcal{F}^{p/d}$ and \mathcal{F}^s , *i.e.* the protein/derivative and solvent structure factors, respectively. We can express each of them as a linear combination

$$\begin{aligned}\mathcal{F}^{p+s} &= a_p^{p+s} \mathcal{F}^p + a_s^{p+s} \mathcal{F}^s, \\ \mathcal{F}^{d+s} &= a_d^{d+s} \mathcal{F}^d + a_s^{d+s} \mathcal{F}^s.\end{aligned}\tag{1}$$

Actually if we knew the a_j^i parameters we would solve the problem at a once by classical methods. Unfortunately this is not the case and the problem turns out to be much more difficult.

Under the hypothesis of statistical independence of the $\mathcal{F}^{p,s}$ structure factor phase differences, *i.e.* $\langle \cos(\phi^s - \phi^p) \rangle \simeq 0$ [2], we can write

$$\begin{aligned}\mathcal{I}^{p+s} &= a_p^{p+s}{}^2 \mathcal{I}^p + a_s^{p+s}{}^2 \mathcal{I}^s, \\ \mathcal{I}^{d+s} &= a_d^{d+s}{}^2 \mathcal{I}^d + a_s^{d+s}{}^2 \mathcal{I}^s \approx a_d^{d+s}{}^2 \mathcal{I}^p + a_s^{d+s}{}^2 \mathcal{I}^s,\end{aligned}\tag{2}$$

where $\mathcal{I}^{p,s} \propto \langle |\mathcal{F}^{p,s}|^2 \rangle$ is the resolution shell averaged intensity and the approximation in the last equation written above is justified by the isomorphism among the protein and its derivatives. a_j^i are some parameters that depend on the hidden variables of the problem. Of course we are interested in spotting the two original sources \mathcal{I}^p and \mathcal{I}^s by using only the recorded signals \mathcal{I}^{p+s} and \mathcal{I}^{d+s} .

Using some information about the statistical properties of the original signals \mathcal{I}^p and \mathcal{I}^s is a possible approach to estimate the a_j^i parameters. The *statistical independence* of the two sources is not surprising whereas the fact that the above condition is not only necessary but also sufficient is [12].

The Independent Component Analysis is a technique recently developed to estimate the a_j^i parameters based on the information of the statistical independence of the original sources. It allows to separate the latter ones from their mixtures \mathcal{I}^{p+s} and \mathcal{I}^{d+s} .

Several applications of ICA have been recently devised and, therefore, a unified mathematical framework is required. To begin with, we rigorously define ICA [13, 14] by referring to a statistical "latent variables" model, *i.e.*

$$x_j \stackrel{def.}{=} a_j^1 s_1 + a_j^2 s_2 + \dots + a_j^n s_n , \quad (3)$$

where j runs over the number of linear mixtures we observe and n is the number of hidden sources.

The statistical model defined in eq.(3) is called Independent Component Analysis. It describes the generation of observed data x_j as a result of an unknown mixture a_j^i of unknown sources s_i . Finding out both the mixing matrix and the hidden sources is the aim of this method. In order to do so, ICA assumes that

- 1) the components s_i are statistically independent,
- 2) the components s_i are random variables and their distribution is not gaussian,
- 3) the mixing matrix a_j^i is square, although this hypothesis can be sometimes relaxed. For a detailed discussion see [12].

Let us suppose that the mixing matrix a_j^i has been computed; the inverse mixing matrix w_i^j is achievable and the problem is readily solved: $s_i = w_i^1 x_1 + w_i^2 x_2 + \dots + w_i^n x_n$ for each hidden source.

Adding some noise terms in the measurements is certainly a more realistic approach although it turns out to be more tricky: For the time being, we shall skip this aspect in order to focus on a free-noise ICA model. Of course extending the conclusions to more complicated models is straightforward.

Without loss of generality we shall assume that x_j are standardized random variables, *i.e.* $Variance(x_j) = 1$, $Mean(x_j) = 0$. The latter choice is always possible since both $Variance$ and $Mean$ are known for the starting data samples x_j . Indeed, we can always replace the starting set of random variables x_j with the new one as follows

$$\tilde{x}_j \stackrel{def.}{=} \frac{x_j - Mean(x_j)}{\sqrt{Variance(x_j)}} . \quad (4)$$

Moreover ICA aims to disentangle the hidden sources (s_i) and, therefore, looking at preprocessing techniques to uncorrelate the *would-be* sources before applying any ICA algorithm is a major advantage. Therefore this procedure, named data whitening, is certainly a useful preprocessing strategy in ICA. The eigenvalue decomposition (EVD) is the most popular way to whiten data: The starting set of variables is linearly transformed according to the following rule

$$\dot{x}_j \stackrel{def.}{=} \left(\frac{V_j^1 V_1^1}{\sqrt{\lambda_1}} + \frac{V_j^2 V_2^1}{\sqrt{\lambda_2}} + \dots + \frac{V_j^n V_n^1}{\sqrt{\lambda_n}} \right) x_1 + \dots + \left(\frac{V_j^1 V_1^n}{\sqrt{\lambda_1}} + \frac{V_j^2 V_2^n}{\sqrt{\lambda_2}} + \dots + \frac{V_j^n V_n^n}{\sqrt{\lambda_n}} \right) x_n , \quad (5)$$

where λ_j and $\{V_j^i\}_{i=1,\dots,n}$ are, respectively, the eigenvalues and the eigenvectors of the n -rank covariance matrix for the starting set of statistical variables. The covariance matrix for the new set of \dot{x}_j variables is diagonal.

Of course the data whitening modifies the mixing matrix a_j^i ; infact, by applying the ICA definition of the eq.(3) to both sets of variables (x_j and \dot{x}_j) in the eq.(5), we get

$$\dot{a}_j^i \stackrel{def.}{=} \left(\frac{V_j^1 V_1^1}{\sqrt{\lambda_1}} + \frac{V_j^2 V_2^1}{\sqrt{\lambda_2}} + \dots + \frac{V_j^n V_n^1}{\sqrt{\lambda_n}} \right) a_1^i + \dots + \left(\frac{V_j^1 V_1^n}{\sqrt{\lambda_1}} + \frac{V_j^2 V_2^n}{\sqrt{\lambda_2}} + \dots + \frac{V_j^n V_n^n}{\sqrt{\lambda_n}} \right) a_n^i , \quad (6)$$

where i runs over $1,\dots,n$. It turns out that data whitening has considerably simplified the initial problem since the new mixing matrix \dot{a}_j^i is orthogonal and, therefore, the n^2 components of a_j^i have been reduced to $n(n-1)/2$.

After having standardized and whitened the starting set of statistical variables, we are ready to implement the ICA algorithm.

Actually we are looking for a unique matrix \dot{w}_i^j that combines with the \dot{x}_j variables in order to get the hidden sources \dot{s}_i satisfying the ICA prescriptions. Indeed the conditions 1),3) of ICA are readily achieved as soon as we note that the product of the whitened set of standardized random variables \dot{x}_j by any n -dimensional orthogonal matrix leaves the variables uncorrelated, whitened, standardized and, moreover, it leaves the mixing matrix \dot{a}_j^i orthogonal.

Therefore we shall limit ourselves to an n -dimensional orthogonal matrix \hat{w}_i^j and we shall fix its $n(n-1)/2$ degrees of freedom by assuming the nongaussianity of the probability distribution functions of the hidden sources $\hat{s}_i = \hat{w}_i^1 \hat{x}_1 + \hat{w}_i^2 \hat{x}_2 + \dots + \hat{w}_i^n \hat{x}_n$.

There are several measures of nongaussianity and a full discussion is beyond the scope of this paper (for more details see [12]); instead we briefly introduce the measure of nongaussianity we shall adopt: The negentropy. Entropy is a fundamental concept of information theory. The entropy of a random variable is its coding length (for details see [15, 16]). For a discrete random variable, entropy is defined as follows

$$\mathcal{H}(Y) \stackrel{def.}{=} - \sum_i P(Y = \xi_i) \log P(Y = \xi_i) , \quad (7)$$

where ξ_i are the possible values of Y . One of the main result of the information theory is that a gaussian variable has the largest entropy among the random variables with the same *Variance*. Therefore we argue that the less structured is a random variable the more gaussian is its distribution. In order to get a nonnegative measure of a random variable nongaussianity, whose value is zero for a gaussian variable, it is worth to introduce the following quantity

$$\mathcal{J}(Y) \stackrel{def.}{=} \mathcal{H}(Y_{gauss.}) - \mathcal{H}(Y) , \quad (8)$$

where $\mathcal{H}(Y_{gauss.})$ is the entropy of a gaussian random variable. Hereafter we shall refer to the eq.(8) as to the negentropy of a random variable Y .

The negentropy of a random variable, as defined in the eq.(8), is well defined by the statistical theory and, moreover, it can be easily generalized to a system of random variables: Infact the additivity of the entropy is immediately extended to the negentropy. Moreover negentropy is invariant under an invertible linear transformation [13, 17]. The major drawback of the negentropy, as defined in the eq.(8), is the computation itself since the precise evaluation of it requires the nonparametric estimation of the probability distribution function for the random variable we are dealing with. Several simplifications of negentropy have been devised and we shall focus on two of them.

i. The kurtosis [18].

The kurtosis is the 4th order momentum of a random variable probability distribution function, *i.e.* $kurtosis(Y) \stackrel{def.}{=} Mean(Y^4)/Mean(Y^2)^2 - 3$, where Y is a random variable. For a gaussian random variable kurtosis equals 0. The negentropy of eq.(8) is readily simplified: $\mathcal{J}(Y) \approx \frac{1}{12} Mean(Y^3)^2 + \frac{1}{48} kurtosis(Y)^2$.

The major drawback of the kurtosis approximation of negentropy is the lack of robustness, since its computation out of a data sample can be very sensitive to the outliers [19].

ii. Maximum entropy [20].

In order to step over the unrobustness of the negentropy approximation described above, it is useful to introduce a conceptually simple and fast to be computed approximation of the negentropy based on maximum entropy principle. We write the negentropy according to the following formula

$$\mathcal{J}(Y) \approx \sum_{j=1}^N c_j [Mean(C_j(Y)) - Mean(C_j(Y_{gauss.}))]^2 , \quad (9)$$

where c_j are suitable coefficients, C_j are nonquadratic functions, Y is a unit variance random variable and $Y_{gauss.}$ is a unit variance gaussian random variable. The approximation of eq.(9) generalizes the kurtosis one; infact for a single function C_j (*i.e.* $N=1$) the choice $C_1 = Y^4$ exactly leads to the kurtosis approximation described above. The slower is the growing of the C_j functions the more robust is the approximation of the negentropy.

Both of the approximations described above satisfy the main features of the negentropy, *i.e.* the nonnegativity, the zero value for a gaussian random variable and the additivity.

Before showing the details of the ICA application to the protein crystallography, we spot some intrinsic ambiguities of the ICA procedure [17].

- a) The *Variance* of the independent components cannot be determined since the hidden sources and the mixing matrix are unknown and they can be simultaneously scaled by the same quantity without modifying any conclusion. The choice $Variance(Y) = 1$ leaves the ambiguity of the sign.
- b) The order of the independent components cannot be determined. Indeed any permutation of the hidden sources leads to a similarity transformation on the mixing matrix and since both of them are unknown the permutation does not affect the algorithm itself.

The ambiguities described above can be solved by means of physical constraints featuring the ICA solutions of the specific problem. We will discuss how to overcome this problem in the next section.

RESULTS AND DISCUSSION

We have focused on the 2-dimensional problem described in the introduction and briefly formalized at the beginning of the theory section.

After having recalled the definitions of the eq.(2), we proceed with the standardizing and the whitening procedures of the starting set of random variables

$$\mathbf{I}^{p/d+s} \xrightarrow{\text{standardizing}} \tilde{\mathbf{I}}^{p/d+s} \xrightarrow{\text{whitening}} \hat{\mathbf{I}}^{p/d+s} \stackrel{\text{def.}}{=} [\mathcal{A}_{wh.} \cdot \tilde{\mathbf{I}}]^{p/d+s}, \quad (10)$$

where $\mathcal{A}_{wh.}$ is the whitening matrix defined by the eigenvalue decomposition (EVD) of the $\tilde{\mathbf{I}}$ *Covariance* matrix.

At this stage we apply the ICA algorithm to $\hat{\mathbf{I}}^{p/d+s}$. In two dimensions an orthogonal matrix is determined by a single angle parameter; we get

$$\mathcal{A}_{ICA}(\theta) \stackrel{\text{def.}}{=} \begin{pmatrix} \cos \theta & -\sin \theta \\ \sin \theta & \cos \theta \end{pmatrix} \longrightarrow \begin{pmatrix} \hat{\mathbf{I}}^p(\theta) \\ \hat{\mathbf{I}}^s(\theta) \end{pmatrix} \stackrel{\text{def.}}{=} \mathcal{A}_{ICA}(\theta) \cdot \mathcal{A}_{wh.} \cdot \begin{pmatrix} \tilde{\mathbf{I}}^{p+s} \\ \tilde{\mathbf{I}}^{d+s} \end{pmatrix}, \quad (11)$$

where the last formula of the eq.(11) defines the θ -dependent solutions of ICA, *i.e.* the standardized, whitened random variables depending on the single parameter θ that has to be fixed by maximizing the total negentropy $\mathcal{J}(\theta)$ as follows

$$\mathcal{J}(\theta) \stackrel{\text{def.}}{=} \mathcal{J}(\hat{\mathbf{I}}^p(\theta)) + \mathcal{J}(\hat{\mathbf{I}}^s(\theta)) \quad \text{maximum}, \quad (12)$$

where we use a single function C_j (*i.e.* $N=1$ in the eq.(9)) and, according to [12], we adopt $C_1(Y) = -\exp(-Y^2/2)$. In the eq.(12) the negentropy additivity has been applied. Other choices for C_1 are possible [12] and we have checked that neither the solutions nor the algorithm are sensitive to them.

We denote with θ_{max} the angle θ where the total negentropy $\mathcal{J}(\theta)$ attains its maximum. Therefore we can conclude

$$\mathcal{A}_{ICA}(\theta_{max}) = \begin{pmatrix} \dot{a}_p^{p+s} & \dot{a}_s^{p+s} \\ \dot{a}_p^{d+s} & \dot{a}_s^{d+s} \end{pmatrix}^{-1}; \quad (13)$$

in that respect $\hat{\mathbf{I}}^{p/s}(\theta_{max})$ are the standardized, whitened and maximally nongaussian random variables corresponding to the hidden sources of the initial problem.

As to the ambiguities of this technique, mentioned at the end of the previous section, we solve the first one by taking the absolute value of $\hat{\mathbf{I}}^{p/s}(\theta_{max})$, *i.e.* we introduce the quantities $\mathcal{I}^{p/s} \stackrel{\text{def.}}{=} |\hat{\mathbf{I}}^{p/s}(\theta_{max})|$.

At this stage we define the protein/solvent fraction as follows

$$f^{p/s} \stackrel{\text{def.}}{=} \frac{\sum_j \Delta \rho_j \mathcal{I}_j^{p/s}}{\sum_j \Delta \rho_j [\mathcal{I}_j^p + \mathcal{I}_j^s]}, \quad (14)$$

where j runs over the number of resolution shells according to eq. (2) and $\Delta \rho_j = \langle \rho \rangle_{j+1} - \langle \rho \rangle_j$, being $\langle \rho \rangle$ the shell averaged resolution.

The protein fraction definition of eq.(14) is justified by the kinematic theory [21] stating that the diffraction intensity is expected to depend on the crystal volume Ω and on the unit cell volume V according to the Ω/V^2 ratio.

According to [22] the relevant information of the protein structures is contained in three resolution ranges, $\leq 1.2\text{\AA}$, $1.7 - 3.0\text{\AA}$ and $\geq 3.5\text{\AA}$. The first range information is dominated by the protein structure at atomic level while in

the third one the solvent content is overwhelming (the Density Modification procedures aim to re-scale the structure factors moduli in the low resolution range to account for the bulk disordered solvent). The scattering powers of protein and solvent are of the same order in the $1.7 - 3.0\text{\AA}$ range [2]. Hence the expression (14) is evaluated in this range. The comparison between the protein fraction value obtained by ICA with the one by Matthews' method [1], computed as in [23], finds out the correct order of the independent components $\mathcal{I}^{P/s}$.

The results of this comparison are shown in Table I for several proteins. The agreement between the protein fractions obtained by the two methods is quite satisfactory.

The proteins reported in Table I are named according to their codes. For each of them we have the crystallographic data of the native and of one derivative for the isomorphous derivative technique. For the anomalous dispersion technique, we use the crystallographic data of the native collected at one wavelength.

On the last row in the Table I the errors are the protein fraction *Variances* for the two different methods. The average values as well as the *Variances* are comparable.

In Fig.1 we report the protein fraction distribution for the proteic structures listed in Table I and computed by ICA. Figure 2 shows the corresponding distribution of the crystal volume per unit of protein molecular weight calculated according to the formula in ref.[1] (for a full comparison see Fig.2 in the reference [1]). According to our analysis the most probable value for the crystal volume per unit of protein molecular weight falls into the range $1.85\text{-}2.25\text{\AA}^3/\text{Dalton}$.

CONCLUSIONS

In this paper we have applied a new technique, the Independent Component Analysis, to calculate the protein fraction out of crystallographic data. The analysis here presented aims to disentangle the protein and the disordered solvent contributions. Provided a sufficient number of crystallographic data (at least as many as the supposed hidden sources), this method has given convincing results, as compared to available ones in the literature. It is a promising tool to investigate some features of protein structures even if its applicability as a robust guideline at the future protein crystallography refinement programs deserves a deeper investigation.

We quote some possible directions of research:

1. Phasing procedures. Indeed weighting the protein structure factors according to the resolution shells of the crystallographic data could provide a crucial improvement of the relevant formulas for the protein phasing procedure implemented in the most popular crystallography refinement programs.
2. Disentangling crystallized and disordered solvent contributions out of the crystal forms of proteins. Infact the larger is the number of the independent crystallographic data referring to the same protein structure, the larger is the number of hidden sources this method can account for, the more precise is the determination of the single hidden source out of the recorded signals.
3. Model independence of ICA results in protein crystallography.

-
- [1] Matthews BW. Solvent Content of Protein Crystals. *J Mol Biol* 1968;33:491–497.
 - [2] Kostrewa D. Bulk Solvent Correction: Practical Application and Effects in Reciprocal and Real Space. *CCP4 Newsletter* 2002;34:1–13.
 - [3] Kostrewa D, Winkler FK. Mg²⁺ Binding to the Active Site of *EcoRV* Endonuclease: A Crystallographic Study of Complexes with Substrate and Product DNA at 2Å Resolution. *Biochemistry* 1995;34:683–696.
 - [4] Cowtan K. <http://www.yorvic.york.ac.uk/~cowtan/fourier/fourier.html>.
 - [5] Andersson KM, Hovmöller S. The protein content in crystals and packing coefficients in different space groups *Acta Crystallographica D* 2000;56:789–790.
 - [6] Li F, Steitz TA. A novel method of determining the number of macromolecules per asymmetric unit from accurate crystal-volume measurements *Acta Crystallographica D* 2003;59:1793–1796.
 - [7] Moews PC, Kretsinger RH. Refinement of the Structure of Carp Muscle Calcium-binding Parvalbumin by Model Building and Difference Fourier Analysis. *J Mol Biol* 1975;91:201–228.
 - [8] Urzhumtsev AG, Podjarny AD. On the problem of Solvent Modelling in Macromolecular Crystal using Diffraction Data: 1. The Low Resolution Range. *CCP4 Newsletter* 1995;31:12–16.
 - [9] Dodson E, Moore M, Ralph A, Bailey S. Macromolecular Refinement. *Proceedings of the CCP4 1996, DL-CONF-96-001*.
 - [10] Jiang JS, Bruenger AT. Protein Hydration Observed by X-ray Diffraction. *J Mol Biol* 1994;243:100–115.
 - [11] Giacovazzo C. *Direct Phasing in Crystallography*. New York: Oxford University Press;1998. 551 p.
 - [12] Hyvärinen A, Oja E. Independent Component Analysis: Algorithms and Applications. *Neural Networks* 2000;13:411–430.
 - [13] Comon P. Independent component analysis - a new concept? *Signal Processing* 1994;36:287–314.
 - [14] Jutten C, Hérault J. Blind separation of sources, part I: An adaptive algorithm based on neuromimetic architecture. *Signal Processing* 1991;24:1–10.
 - [15] Cover TM, Thomas JA. *Elements of Information Theory*. New York: John Wiley & Sons; 1991.
 - [16] Papoulis A. *Probability, Random Variables and Stochastic Processes*. New York: McGraw–Hill; 1991.
 - [17] Hyvärinen A. Survey on independent component analysis. *Neural Computing Surveys* 1999;2:94–128.
 - [18] Jones MC, Sibson R. What is projection pursuit ? *J of the Royal Statistical Society, ser A* 1987;150:1–36.
 - [19] Huber PJ. Projection Pursuit. *The Annals of Statistics* 1985;13:435–475.
 - [20] Hyvärinen A. New approximations of differential entropy for independent component analysis and projection pursuit. *Advances in Neural Information Processing Systems* 1998;10:273–279.
 - [21] Authier A. *Dynamical Theory of X-Ray Diffraction*. New York: Oxford University Press;2001. 57 p.
 - [22] Morris RJ, Bricogne G. Sheldrick's 1.2 Å rule and beyond. *Acta Crystallographica D* 2003;59:615–617.
 - [23] Kantardjef K, Rupp B. Matthews coefficient probabilities: Improved estimates for unit cell contents of proteins, DNA, and protein-nucleic acid complex crystals. *Protein Science* 2003;12:1865–1871.
 - [24] Moore MH, Gulbis JM, Dodson EJ, Demple B, Moody PCE. Crystal-structure of a suicidal DNA-repair protein - the ADA O6-methylguanine- DNA methyltransferase from *Escherichia coli*. *Embo Journal* 1994;13:1495–1501.
 - [25] Toro I, Basquin J, Teo–Dreher H, Suck D. Archaeal SM proteins form heptameric and hexameric complexes: crystal structures of the SM1 and SM2 proteins from the hyperthermophile *archaeoglobus fulgidus*. *J Mol Biol* 2002;320:129.
 - [26] Mattevi A, Obmolova G, Schulze E, Kalk KH, Westphal AH, De Kok A, Hol WGJ. The atomic structure of the cubic core of the pyruvate dehydrogenase complex. *Science* 2002;255:1544–1550.
 - [27] Hofmann B, Budde H, Bruns K, Guerrero SA, Kalisz HM, Menge U, Montemartini M, Nogoceke E, Steinert P, Wissing JB, Flohe L, Hecht HJ. Structure of Tryparedoxins revealing interaction with Trypanothione. *Biol Chem* 2001;382:459.
 - [28] Spallarossa A, Donahue J, Larson T, Bolognesi M, Bordo D. *Escherichia Coli* GLPE is a Prototype Sulfurtransferase for the single-domain Rhodanese Homology Superfamily. *Structure Fold Des* 2001;9:1117.
 - [29] Glover I, Haneef I, Pitts J, Woods S, Moss D, Tickle I, Blundell TL. Conformational flexibility in a small globular hormone: x-ray analysis of avian pancreatic polypeptide at 0.98Å resolution. *Biopolymers* 1983;22:293–304.
 - [30] Cedergren–Zeppezauer ES, Larsson G, Nyman PO, Dauter Z, Wilson KS. The X-ray structure of a dUTPase. *Nature* 1992;355:740–743.
 - [31] Hecht H, Sobek H, Haag T, Pfeifer O, Van Pee KH. The metal-ion-free oxidoreductase from *Streptomyces aureofaciens* has an a/b hydrolase fold. *Nature Struct Biol* 1994;1:532–537.
 - [32] Dauter Z, Wilson KS, Sieker LC, Meyer J, Moulis JM. Atomic resolution (0.94Å) structure of *Clostridium acidurici* ferredoxin. Detailed geometry of [4Fe-4S] clusters in a protein. *Biochemistry* 1997;36:16065–16073.
 - [33] Dauter Z, Dauter M, de La Fortelle E, Bricogne G, Sheldrick GM. Can Anomalous Signal of Sulfur Become a Tool for Solving Protein Crystal Structures ? *J Mol Biol* 1999;289:83–92.
 - [34] Matak–Vinkovic D, Vinkovic M, Saldanha SA, Ashurst JA, Von Delft F, Inque T, Miguel RN, Smith AG, Blundell TL, Abell C. Crystal Structure of *Escherichia Coli* Ketopantoate Reductase at 1.7Å resolution and insight into the Enzyme mechanism. *Biochemistry* 2001;40:14493..
 - [35] Hecht HJ, Erdmann H, Park KJ, Sprinzl M, Schmid RD. Crystal Structure of NADH Oxidase from *Thermus Thermophilus*. *Nature Struct Biol* 1995;2:1109–1114.

TABLE I: Numerical values for protein fractions. The third column refers to our method, the fourth column refers to Matthews' method [1]. The protein fraction calculated by ICA is averaged on the whole crystallographic data resolution range. SIR, MIR, SAD and MAD refer to the diffraction technique adopted to collect data. On the last column we report the error estimate between the two methods.

<i>protein</i>	<i>technique</i>	<i>prot. frac.</i> (<i>this paper</i>)	<i>prot. frac.</i> (<i>Matthews</i> [1])	<i>err.</i>
<i>GMT (Ortho)</i> [24]	<i>SIR</i>	0.31	0.30	0.03
<i>GMT (Mono)</i> [24]	"	0.57	0.53	0.07
<i>SM₂</i> [25]	"	0.68	0.65	0.05
<i>E₂</i> [26]	"	0.33	0.26	0.24
<i>TXN</i> [27]	"	0.44	0.45	0.02
<i>GLPE</i> [28]	"	0.69	0.61	0.12
<i>APP</i> [29]	"	0.65	0.67	0.03
<i>dUTPase</i> [30]	<i>MIR</i>	0.40	0.37	0.08
<i>BPO</i> [31]	"	0.45	0.44	0.02
<i>CAUFD</i> [32]	<i>SAD</i>	0.79	0.86	0.08
<i>LYSO₂</i> [33]	"	0.61	0.58	0.05
<i>KPR</i> [34]	<i>MAD</i>	0.53	0.54	0.02
<i>NOX</i> [35]	"	0.60	0.51	0.16
<i>average</i>		0.54 ± 0.15	0.52 ± 0.16	0.07

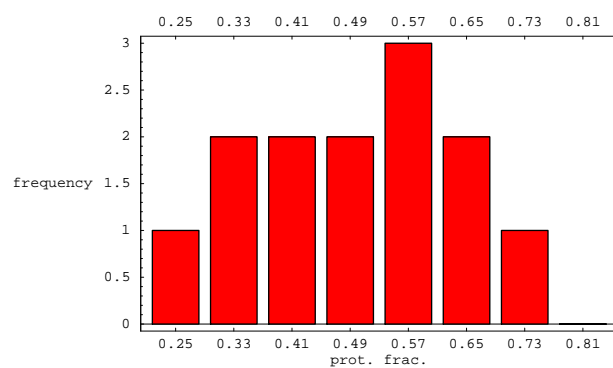


FIG. 1: Protein fraction distribution for the proteic structures listed in Table I computed by ICA.

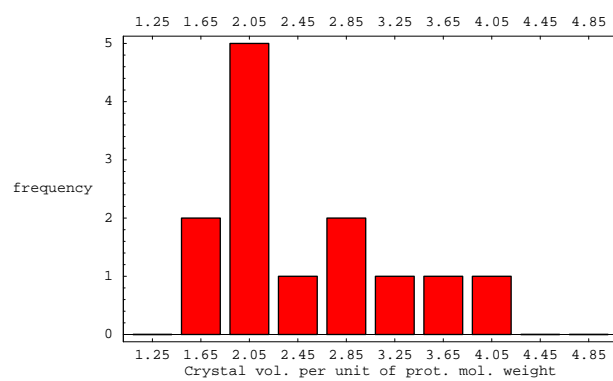


FIG. 2: Crystal volume per unit of protein molecular weight distribution for the proteic structures listed in Table I computed by ICA (for a comparison see Fig.2 in ref.[1]). x-axis units are $\text{\AA}^3/\text{Dalton}$.